Validation of a Real-Time Capable Multibody Vehicle Dynamics Formulation for Automotive Testing Frameworks Based on Simulation

ALBERTO PARRA[1,2], **ANTONIO J. RODRíGUEZ**[3],
ASIER ZUBIZARRETA[2], **(Member, IEEE), AND JOSHUÉ PÉREZ**[1], **(Member, IEEE)**

[1]TECNALIA, Basque Research and Technology Alliance (BRTA), 48160 Derio, Spain
[2] Department of Automatic Control and System Engineering, Faculty of Engineering of Bilbao, University of the Basque Country UPV/EHU, 48013 Bilbao, Spain
[3]Laboratory of Mechanical Engineering, University of A Coruna, 15403 Ferrol, Spain

Corresponding author: Alberto Parra (alberto.parra@tecnalia.com)

ABSTRACT The growing functionalities implemented on vehicles have increased the importance of simulation in the design process. This complexity is mainly driven by the introduction of electrified power-trains, Advanced Driver Assistance Systems (ADAS) and Automated Driving Systems (ADS). Additionally, the automotive industry must reduce development times and cost, while keeping flexible development capabilities and fulfilling demanding regulation standards for safety-critical systems. Existing testing frameworks based on simulation implement typically analytical models to ensure real-time performance, and provide limited flexibility to perform Hardware in the Loop (HiL) setup based tests. In this work a vehicle modelling approach which guarantees high accuracy and real-time capabilities is proposed. Moreover, the proposed approach is validated firstly with real vehicle data, demonstrating that it can fairly reproduce the behaviour of the vehicle tested; and secondly, in a HiL setup to demonstrate the real-time execution capabilities of the approach.

INDEX TERMS Multibody formulation, vehicle model, vehicle dynamics, ADAS, automotive simulation framework.

I. INTRODUCTION

Over the last decades, technology development has motivated the increase of electronics systems, being the automotive sector one of the main affected. In modern vehicles, functions related to electronics and software are claimed to represent over 90% of the innovations [1] and up to 30% of the cost of a vehicle [2]. In addition, the upcoming rising technologies such as electrified multi-motor propulsion powertrains, Advanced Driver Assistance Systems (ADAS), and automated driving (AD), are certainly further pushing the complexity of these systems to hardly sustainable levels to be handled by traditional approaches [3].

Validation of the aforementioned novel functionalities is a key issue on the safety and certification of future vehicles. However, traditional track-based scenarios, wide-spread in the automotive industry, do not provide enough flexibility to

The associate editor coordinating the review of this manuscript and approving it for publication was Ricardo De Castro.

test different situations. New testing frameworks are required to reduce costs and time to market [3], [4] [5]. Nevertheless, a validation framework based on simulation requires a representative vehicle model. The development of accurate vehicle models has been traditionally associated with the motorsport field, with the so-called "Lap Time Simulators". However, these issues have aroused the interest of the Automotive Industry in the development of accurate vehicle dynamic modelling approaches.

A representative model for vehicle dynamics presents multiple advantages. First, the model can be used to optimize the dynamic performance of the vehicle, simulating multiple configurations and identifying the optimal ones before testing them on tracks, which can effectively reduce the development time especially if the simulations are able to be run faster than real time. Second, it allows testing the vehicle behaviour on critical scenarios in a safe way. Third, it enables the development and testing of control functionalities related to ADAS and Automated Driving, in a wide variety of scenarios, both

in simulation or using Hardware in the Loop (HiL) setups. And finally, it reduces the cost of physical tests, in which real vehicles and hardware are required. In fact, nowadays, validation tests in the real vehicle have been greatly reduced thanks to the possibility of performing HiL based tests [7].

The effectiveness of HiL setups is conditioned by the accuracy of the model and its real-time execution capabilities, whose balance is not trivial. In general, two main approaches have been used to implement vehicle models: analytical models [8]–[10] and multibody ones [11]. The first have been implemented successfully in commercial simulators. However, due to the complex nature of vehicle dynamics, the use of analytical models typically implies neglecting some degrees of freedom and simplifying some dynamic effects. In fact, this is the case of many recent simulation frameworks focused on ADAS/ADS features development (CARLA [15], SYNTHIA [16], SCANeRS studio, Cognata Studio [17] and Virtual Test Drive [18]). These compensate the high computational cost derived from the use of game engines [19] to simulate complex environments and on-board sensors, with a simplified vehicle dynamics model. On the other hand, multibody formulation based models [11]–[14], can represent more accurately vehicle dynamics, but present an increased computational cost that limits their real-time implementation [21], [22], especially if flexible bodies are implemented [20]. Likewise, due to this high computational cost, computationally powerful devices would be needed in order to fulfill the real time requirements.

Additionally, flexibility is also a key issue when HiL tests are to be performed. Nowadays, there are several hardware platforms to implement the developed vehicle models (dSPACE [23], ETAS [24], National Instruments [25], Speed-Goat [26], etc.). However, they usually are integrated with specific developing environments (such as Matlab/Simulink in the case of dSPACE and Speedgoat or LabVIEW in the case of National Instruments hardware), and present compatibility issues when models coming from different developing environments need to be deployed. Therefore, in order to have flexibility regarding the hardware implementation, compatibility has to be considered. In this sense, the developing environments that have turned out to provide greater compatibility are C code based ones [10].

In summary, a proper vehicle dynamics model is mandatory to implement an accurate testing framework based on simulation. This means that the model has to be accurate, computationally efficient and flexible regarding its implementation. However, fulfilling all three aspects is not trivial, and proposed solutions in the literature, to the best of our knowledge, fail to provide all of them.

Hence, this work covers the identified gap, with the following novel contributions:

- Application to vehicle dynamics modelling of a computationally efficient multibody formulation, focused on providing optimal accuracy and real time execution capabilities.

- The proposed formulation is designed to consider flexibility, having been developed in C code for its implementation in different hardware platforms.
- A deep validation, which includes, on the one hand, an accuracy analysis comparing the data provided by the proposed multibody model with those provided by a real vehicle in a wide set of tests, and on the other hand, a validation of the HiL and real time capabilities.

The rest of this work is divided as follows. Section II focuses on the proposed multibody vehicle dynamic model. Section III introduces the test vehicle to be evaluated, a light duty truck, details the set of experiments carried out to validate the modelling approach, and the accuracy analysis carried out by comparing the real and simulated data for four standard maneuvers. Section IV illustrates the real-time capabilities of the proposed approach in an HiL setup. Finally, the most important ideas are summarized.

II. HIGH FIDELITY AND REAL TIME CAPABLE VEHICLE MODELLING APPROACH

As analyzed in the introduction, a representative vehicle model is a key part of a testing framework based on simulation. Analytical models are typically preferred in the proposed simulators in the literature, due to the high computational cost of multibody models, even if the latter can provide better accuracy. Novel multibody formulations have led into more efficient approaches. Based on [29], the proposed formulation is developed in such a way that real-time performance can be achieved on hardware with low computational capabilities. This is an important feature since it allows to use multibody models in several automotive applications [30]. The dynamics of the vehicle used in this work are based on a multibody model with fourteen degrees-of-freedom. Next, the modelling approach will be detailed, where the vehicle, tire, steering, and suspension models are deeply explained.

A. COORDINATES SELECTION

As stated earlier, a multibody approach provides enough accuracy to represent the real vehicle dynamics, although this is achieved at a higher computational cost. However, as the application of the proposed vehicle model is to test automotive control systems, computational efficiency must be considered to provide real-time capabilities.

An efficient multibody simulation depends on several factors: the modelling, the coordinates selected to represent the vehicle, the formulation of the equations of motion and the numerical integrator selected [11].

Regarding the coordinates selection, two types can be chosen: independent or dependent coordinates. On the one hand, adopting independent coordinates means that the number of coordinates coincides with the number of degrees-of-freedom and is therefore minimal, leading to a more efficient simulation. However, they are suitable for the open-loop mechanism, since in systems with closed loops, employing independent coordinates could result in an undetermined

system: the same coordinate value could result in different motions. On the other hand, dependent coordinates are able to define unequivocally the movement of the mechanism, employing a higher number of coordinates. Since they are dependent, they must be related to constraint equations, which increases the computational cost of the simulation [11].

Since the coordinates selected have direct effects on the complexity of the system definition, related to the performance of the multibody model, the methods developed for defining the coordinates can be grouped into global and topological methods [11], [27].

Coordinates employed in global methods define the system in an absolute form. They are general and systematic to implement, but not very efficient since they lead to a high number of variables and constraints equations [28]. In topological methods, the coordinates define each body of the system with respect to its previous body, suggesting to use recursive procedures in order to obtain the motion of each body. These methods lead to a system with a minimum number of dependent coordinates [11].

As presented in [28], using a topological method instead of a global method reduces the cost of simulation, increasing the efficiency, especially in the case of multibody models which involve a high number of variables, as in automotive applications. From the work in [28], an efficient topological method based on recursive techniques is presented.

The proposed approach is based on the method proposed in [29], where using a recursive method [28], the vehicle can be modelled with one coordinate for each degree-of-freedom. Being independent coordinates, the definition of constraint equations is avoided and the computational cost of the simulation can be reduced.

This way, first, the coordinates associated to the chassis frame can be defined. Three Cartesian coordinates of a point in the front part of the car (x, y, z), along with the three Cardan angles of the chassis for the inertial frame of reference $(\alpha\ \beta\ \gamma)$, are selected.

Regarding the suspension system, the front suspension system is considered as independent suspensions and two-degrees-of-freedom are involved: the compression of the spring and the steering. Regarding the modelling, the mechanism of each suspension has closed loops, meaning that using the set of independent coordinates could not represent properly the motion of the suspension. The main approach of [29] overcomes this situation by replacing the suspension mechanism by a new type of joint, known as macrojoint. This joint represents in a table the kinematics of the centre of the knuckle in terms of the Cartesian coordinate for the vertical suspension displacement $\bar{z}_i$ and the steering input.

In the case of the rear suspension system, a rigid axle is considered, and the aforementioned approach is also considered, with no steering input. This way, it is modelled with a Cartesian coordinate for the vertical displacement of the axle centre and an angle that represents the roll movement of the axle ($\bar{z}_{ra}\ \bar{\alpha}_{ra}$). From both coordinates, tables are generated in order to represent the kinematics of the axle.
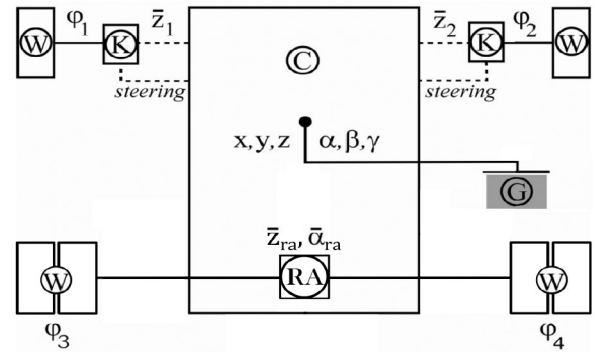

FIGURE 1. Vehicle Multibody Scheme.

Finally, the position of each wheel with respect to the knuckle (in the case of front wheels) and the rigid axle (in the case of rear wheels) is defined by an angle around the wheel axis, ($\varphi = \begin{bmatrix} \varphi_1\ \dots\ \varphi_4 \end{bmatrix}$). It must be noted that, although the rigid axle has four tires, they are grouped under two rotating wheels. Hence, there are two degrees-of-freedom related with the wheel rotation of the rigid axle.

This makes a total of fourteen independent coordinates, which are grouped into vector $\mathbf{z}$ (See Fig. 1). It must be noted that the steering is not included since it is an input to the model and not a coordinate itself.

$$\mathbf{z}^T = \left\{ x\quad y\quad z\quad \alpha\quad \beta\quad \gamma\quad \bar{z}_1\quad \bar{z}_2\quad \bar{z}_{ra}\quad \bar{\alpha}_{ra}\quad \varphi \right\} \quad (1)$$

Finally, the local reference system established for each body has been defined according to the ISO 8855 [32].

B. MULTIBODY FORMULATION
The semi-recursive dynamic formulation proposed in [28], and previously presented by the authors in [31], has been used to derive the equations of motion of the vehicle model. As stated in Section II-A, these kind of formulations based on topological methods allow to define a model with a reduced set of coordinates, increasing the efficiency of the simulation. The main disadvantage of these formulations is that the mass matrix and generalized forces vector are not constant. Nevertheless, the reduced number of coordinates employed usually pays off the computational cost of computing the mass matrix and generalized forces vector each time step, especially with large systems [28].

Although the size of the model employed in this work is not large, the main computational benefit of the presented approach comes from replacing the suspension system with the macro-joint, leading to a formulation in relative coordinates which are independent. Hence, no constraints equations must be considered and the equations of motion will be a set of ordinary differential equations (ODEs), instead of the differential-algebraic system of equations (DAEs), allowing a simpler and more efficient formulation. However, the definition of the equations of motion (expressions for the mass matrix and generalized forces) in relative coordinates is complex. Hence, the interest on the semi-recursive formulation is related with the definition of the equation of motion

in the relative coordinates employed. Being semi-recursive implies that only the kinematics and the assembly of the mass matrix and force vector are computed in a recursive manner. Since the detailed explanation of the employed multibody formulation is out of the scope of this work, it is briefly described hereafter. The reader is referred to [27], [28] for further details.

The semi-recursive formulation defines an alternative set of coordinates, the so-called body coordinates. Using this new set of coordinates, the definition of the dynamic terms of the equation of motion becomes simpler. Body coordinates must be later related with the set of relative coordinates in order to derive the equations of motion in terms of the relative coordinates.

The body coordinates can be expressed for each body at velocity level in the following form,

$$\mathbf{Z} = \left\{ \begin{array}{c} \dot{\mathbf{s}} \\ \omega \end{array} \right\} \tag{2}$$

being $\dot{\mathbf{s}}$ the velocity of the point of the body which at that particular time is coincident with the fixed frame origin, and ω the angular velocity of the body. The relation between the body coordinates (and their time derivatives) of two neighbour bodies is,

$$\mathbf{Z}_i = \mathbf{Z}_{i-1} + \mathbf{b}_i \dot{z}_i \tag{3}$$

$$\dot{\mathbf{Z}}_i = \dot{\mathbf{Z}}_{i-1} + \mathbf{b}_i \ddot{z}_i + \mathbf{d}_i \tag{4}$$

where $\mathbf{b}_i$ and $\mathbf{d}_i$ terms relate the body coordinates with the independent coordinates. Explicit expressions of $\mathbf{b}_i$ and $\mathbf{d}_i$ terms are available for conventional joints [28], and they have been used for the wheels, as they are connected to the knuckles through rotational joints. However, for the knuckles, connected to the chassis using macro-joints, the expressions presented in [29] are used.

Once the evaluation of the whole set of terms is carried out, the relation between the body coordinates $\mathbf{Z}$ that is used in the semi-recursive formulation and the set of independent coordinates $\mathbf{z}$ that define the vehicle is established.

$$\mathbf{Z} = \mathbf{R}\dot{z} \tag{5}$$

$$\dot{\mathbf{Z}} = \mathbf{R}\ddot{z} + \dot{\mathbf{R}}\dot{z} \tag{6}$$

where $\mathbf{R}$ is the matrix that relates the body coordinates and the independent coordinates based on the terms $\mathbf{b}_i$ and $\mathbf{d}_i$ [28].

The equations of motion in body coordinates that describe the dynamics of the vehicle can be projected into the independent relative coordinates, thus yielding,

$$\mathbf{R}^T \bar{\mathbf{M}} \mathbf{R} \ddot{z} = \mathbf{R}^T \left(\bar{\mathbf{Q}} - \bar{\mathbf{M}} \dot{\mathbf{R}} \dot{z} \right) \tag{7}$$

where $\bar{\mathbf{M}}$ and $\bar{\mathbf{Q}}$ are the mass matrix and force vector of the system for body coordinates, whose expressions can be found in [27]. This equation can be reduced to,

$$\mathbf{M}\ddot{z} = \mathbf{Q} \tag{8}$$

being $\mathbf{M}$ and $\mathbf{Q}$ the mass matrix and force vector for the selected set of independent coordinates, which are obtained

in a recursive form, accumulating the body mass matrices and forces from the leaves to the root of the kinematic chain (See Fig. 1) [28]. Their full expressions can be found in [29].

To integrate in time the equations of motion, a structural integrator is selected. Since all the integrators of this family follow a similar scheme, the strategy for combining them with the dynamic equations of the multibody system can be preserved. Thus, it is possible to use different integrators without excessive additional effort. The reader is referred to [27] for the complete set of equations of the structural integrators. In this work, the well-known implicit single-step trapezoidal rule with fixed time step [27] has been adopted. The corresponding difference equations in velocities and accelerations are,

$$\dot{\mathbf{z}}_{n+1} = \frac{2}{\Delta t} \mathbf{z}_{n+1} + \dot{\mathbf{z}}_n^* \tag{9}$$

$$\dot{\mathbf{z}}_n^* = - \left(\frac{2}{\Delta t} \mathbf{z}_n + \dot{\mathbf{z}}_n \right) \tag{10}$$

$$\ddot{\mathbf{z}}_{n+1} = \frac{4}{\Delta t^2} \mathbf{z}_{n+1} + \ddot{\mathbf{z}}_n^* \tag{11}$$

$$\ddot{\mathbf{z}}_n^* = - \left(\frac{4}{\Delta t^2} \mathbf{z}_n + \frac{4}{\Delta t} \dot{\mathbf{z}}_n + \ddot{\mathbf{z}}_n \right) \tag{12}$$

where n represents the time step and Δt is time-step size.

If the previous equations are introduced in the dynamic equation of motion, the resulting system can be expressed as,

$$\mathbf{f}(\mathbf{z}_{n+1}) = \mathbf{0} \tag{13}$$

where $\mathbf{z}_{n+1}$ are the positions at the next time step, which are the unknowns. Since this set of equations is a non-linear system of algebraic equations, the Newton-Raphson iteration procedure can be used to find a solution. Thus,

$$\left. \frac{\partial \mathbf{f}(\mathbf{z})}{\partial \mathbf{z}} \right|_{\mathbf{z} = \mathbf{z}_{n+1,i}} \left(\mathbf{z}_{n+1,i+1} - \mathbf{z}_{n+1,i} \right) = -\mathbf{f} \left(\mathbf{z}_{n+1,i} \right) \tag{14}$$

where the residual vector is,

$$\mathbf{f}(\mathbf{z}) = \frac{\Delta t^2}{4} (\mathbf{M}\ddot{z} - \mathbf{Q}) \tag{15}$$

and the approximated tangent matrix is,

$$\frac{\partial \mathbf{f}(\mathbf{z})}{\partial \mathbf{z}} \simeq \mathbf{M} + \frac{\Delta t}{2} \mathbf{C} + \frac{\Delta t^2}{4} \mathbf{K} \tag{16}$$

where the terms $\mathbf{K}$ and $\mathbf{C}$ represent the contribution of the elastic and damping forces to the tangent matrix respectively. They are defined as,

$$\mathbf{K} = -\partial \mathbf{Q}/\partial \mathbf{z} \tag{17}$$

$$\mathbf{C} = -\partial \mathbf{Q}/\partial \dot{z} \tag{18}$$

The detailed procedure for obtaining $\mathbf{K}$ and $\mathbf{C}$ is presented in [27]. As an example, the contribution of the front suspension spring to the stiffness matrix $\mathbf{K}$ is presented hereafter.

Being $\mathbf{s}$ the spring length and f the force that it exerts, the contribution of the spring to the stiffness matrix $\mathbf{K}$ is,

$$\mathbf{K} = -\mathbf{Q}_\mathbf{z} = -(\mathbf{s}_\mathbf{z}^t f)_\mathbf{z} = -\mathbf{s}_\mathbf{z}^t f_\mathbf{z} = -\mathbf{s}_\mathbf{z}^t f_s \mathbf{s}_\mathbf{z}^t \tag{19}$$

where the second derivative of the distance **s** with respect to **z** twice has been neglected [27]. The derivative of **s** with respect to each relative coordinate z can be obtained by giving unit velocities to the relative coordinates,

$$\mathbf{s}_{\mathbf{z}_j} = \dot{\mathbf{s}}_{(\dot{z}_j=1, \dot{z}_i=0, i \neq j)} \qquad (20)$$

Thus, if the suspension length is defined from a point $\mathbf{r_A}$ to a point $\mathbf{r_B}$, following the direction of the unit vector $\mathbf{u_{AB}}$,

$$\mathbf{s}_{\mathbf{z}_j} = \mathbf{u}_{\mathbf{AB}}^{\mathbf{t}}(\dot{\mathbf{r}}_{\mathbf{B}} - \dot{\mathbf{r}}_{\mathbf{A}})_{(\dot{z}_j=1, \dot{z}_i=0, i \neq j)} \qquad (21)$$

If the suspension spring is linear, the force f can be defined as,

$$f = -k(s - s_0) \qquad (22)$$

where k is the stiffness of the spring and s_0 is its natural length. Then, the derivative of f with respect to **s** is $f_{\mathbf{s}} = -k$ and the contribution of the spring to **K** becomes,

$$\mathbf{K} = \mathbf{s}_{\mathbf{z}}^{t} k \mathbf{s}_{\mathbf{z}}^{t} \qquad (23)$$

The calculation of $\mathbf{s_z}$ can be optimized considering that only the terms related to a coordinate which produces a change in the spring length are different from zero. Thus, with a previous analysis of the topology of the system, the calculations can be minimized. This procedure has been followed to derive the contribution from the other elements of the system to the stiffness and damping matrices, such as the rigid axle or the tires.

It should be noted that, in order to ensure real-time performance, the maximum number of iterations per time step is limited.

Once that $\mathbf{z}_{n+1}$ is known, the positions, velocities and accelerations are obtained for each point and body of the vehicle model, and the dynamics and motion of the vehicle are determined.

C. TIRE MODELLING

Tire modelling is one of the most challenging tasks in vehicle dynamics, as they are a crucial element and their behaviour depend on a high number of parameters. Several approaches have been proposed in the literature, such as structural tire models [33], [34], which require a high computational cost, or those based on empirical data [35]–[37], which are able to provide optimal accuracy while keeping low computational cost. Therefore, in this work, Pacejka's 2006 'Magic Formula' semi-empirical approach has been implemented [37] where the tire is characterized by a set of coefficients. This model enables real-time implementation of robust tire-road contact force and moment calculations for steady-state and transient tire behaviour, using longitudinal, lateral, turn slip, wheel inclination angle and vertical forces as input quantities.

The ground is defined by a triangular mesh, whose elements size can be modified to increase the precision in the obstacles of the terrain, such as bumps. This mesh will be employed during the simulation to determine parameters as
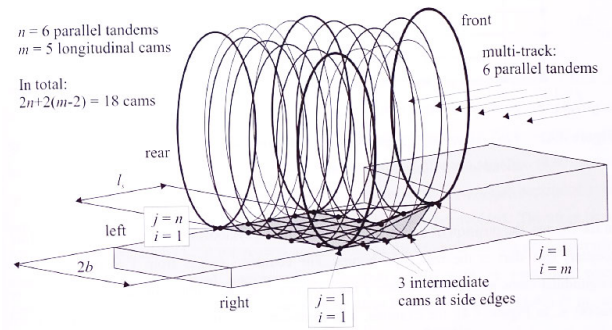

FIGURE 2. Ellipses model for tire contact point [38].

the contact point, the normal direction of the terrain and the indentation of the tire into the terrain. These parameters are required to reach a correct road-vehicle interaction during the simulation.

The contact point is obtained through a boundary volume around the wheel: any element of the mesh inside the boundary volume is considered to the definition of the contact plane. The contact plane determines the deformation of the tire and, therefore, an accurate calculation is critical, specially when the vehicle is over an obstacle. The method presented in [38] proposes to project a set of ellipses from the wheel center into the selected elements of the mesh. The intersection points between ellipses and mesh are employed to define a plane, from where a mean value of the normal direction of the contact is obtained. At a final step, the indentation of the tire into the normal direction is calculated, which is employed in the Pacejka model together with the normal direction of the plane to obtain the magnitude and direction of the tire forces.

D. STEERING AND SUSPENSION SYSTEM

Both the kinematics and dynamics of the suspension system, are modelled using look-up tables tables. These tables can be generated by using a multibody model of the suspension system or by experimental data, as detailed in Section III-A.

The dynamics related elements of the suspension, such as the springs and dampers, are modelled as tables where the force is related with the suspension deflection and velocity of deflection respectively. Each element has been characterized experimentally, as stated in Section III-A.

Regarding the front suspension system, an off-line kinematic analysis allows determining the position of the centre of the knuckle for a particular range of values of the steering and vertical spring displacement. Thus, for each steering position, the vertical displacement of the spring is modified from the top to the bottom of the vertical motion of the suspension, obtaining the position of the centre of the knuckle for each pair of steer and spring compression values. Once that the positions for the entire range of movement of the suspension are gathered, the velocities and accelerations are derived through numerical differentiation of the positions.

Due to the particularities of the macro-joints substituting the suspension links, special calculations should be

performed to obtain the positions, velocities and accelerations of the knuckle [29].

Thus, the coordinates of the origin of the knuckle (for knuckle i, with suspension coordinate $\bar{z}_1$), $\mathbf{r_k}$, is obtained as,

$$\mathbf{r_k} = \mathbf{r_c} + \mathbf{R_c}\bar{\mathbf{r}}_\mathbf{k} \qquad (24)$$

$\mathbf{r_c}$ is the vector of coordinates of the origin of the chassis local reference frame, (x, y, z), $\mathbf{R_c}$ is the chassis rotation matrix, function of (α, β, γ), and $\bar{\mathbf{r}}_\mathbf{k}$ is the local position (with respect to the chassis reference frame) of the origin of the knuckle. This value is obtained from the kinematic table for a value of $\bar{z}_1$ and a certain steering angle.

The expressions for the velocity of the origin of the knuckle, $\mathbf{v}_k$,

$$\mathbf{v_k} = \mathbf{v_c} + \omega_\mathbf{c} \times (\mathbf{r_k} - \mathbf{r_c}) + \mathbf{R_c}\frac{d\bar{\mathbf{r}}_\mathbf{k}}{d\bar{z}_1}\dot{\bar{z}}_1 \qquad (25)$$

where $\mathbf{v_c}$ is the velocity of the chassis frame and ω_c is the chassis angular velocity. The three components of the derivative of $\bar{\mathbf{r}}_\mathbf{k}$ with respect to $\bar{z}_1$ are tabulated as function of $\bar{z}_1$ and the steering angle. The knuckle angular velocity, ω_k, is,

$$\omega_\mathbf{k} = \omega_\mathbf{c} + \mathbf{R_c}\bar{\omega}_\mathbf{k/c} \qquad (26)$$

being $\bar{\omega}_\mathbf{k/c}$ the angular velocity of the knuckle with respect to the chassis,

$$\bar{\omega}_\mathbf{k/c} = \begin{bmatrix} 1 & 0 & sin\,\bar{\beta} \\ 0 & cos\,\bar{\alpha} & -sin\,\bar{\alpha}\,cos\,\bar{\beta} \\ 0 & sin\,\bar{\alpha} & cos\,\bar{\alpha}\,cos\,\bar{\beta} \end{bmatrix}\frac{d\bar{\theta}_\mathbf{k}}{d\bar{\mathbf{z}}_\mathbf{1}}\dot{\bar{z}}_\mathbf{1} \qquad (27)$$

where $\bar{\theta}_\mathbf{k}$ are the orientation angles of the knuckle, whose value is also included in the kinematic tables as a function of $\bar{z}_1$ and the steering angle.

The acceleration of the origin of the knuckle, $\mathbf{a}_k$,

$$\mathbf{a_k} = \mathbf{a_c} + \alpha_\mathbf{c} \times (\mathbf{r_k} - \mathbf{r_c}) + \omega_\mathbf{c} \times [\omega_\mathbf{c} \times (\mathbf{r_k} - \mathbf{r_c})]$$
$$+ 2\omega_\mathbf{c} \times \mathbf{R_c}\frac{d\bar{\mathbf{r}}_\mathbf{k}}{d\bar{z}_1}\dot{\bar{z}}_1 + \mathbf{R_c}\left(\frac{d\bar{\mathbf{r}}_\mathbf{k}}{\dot{\bar{z}}_1}\ddot{\bar{z}}_1 + \frac{d^2\bar{\mathbf{r}}_\mathbf{k}}{d\bar{z}_1^2}\dot{\bar{z}}_1^2\right) \qquad (28)$$

where $\mathbf{a_c}$ is the acceleration of the chassis frame and $\alpha_\mathbf{c}$ is the chassis angular acceleration. The three components of the second derivative of $\bar{\mathbf{r}}_\mathbf{k}$ with respect to $\bar{z}_1$ are tabulated as function of $\bar{z}_1$ and the steering angle. The knuckle angular acceleration, $\alpha_\mathbf{k}$, is,

$$\alpha_\mathbf{k} = \alpha_\mathbf{c} + \mathbf{R_c}\bar{\alpha}_\mathbf{k/c} + \omega_\mathbf{c} \times \mathbf{R_c}\bar{\omega}_\mathbf{k/c} \qquad (29)$$

being $\bar{\alpha}_\mathbf{k/c}$ the angular acceleration of the knuckle with respect to the chassis, obtained as the time derivative of $\bar{\omega}_\mathbf{k/c}$.

Additional parameters for the front suspension can be adapted to its behaviour. Different deflections of the spring can be considered through the motion ratio of the suspension. Also different compliance coefficients have been included, as the relation of the toe, camber and longitudinal displacement of the suspension with the longitudinal force; the effects of the steer, inclination of the suspension and lateral displacement on the lateral forces; and the steer and inclination influence on the steering torque of the wheel.

TABLE 1. Vehicle parameters.

Mass (kerb) [kg]	2067
Mass (test condition) [kg]	3267
Wheelbase [m]	3.725
Front Axle Distance to CoG [m]	1.162
CoG height [m]	0.716
Front Axis Track [m]	1.745
Rear Axis Track [m]	1.545
Tire Radius [m]	0.349
Frontal Area [m]	3.8
Drag Coefficient	0.7
Rolling resistance Coefficient	0.009
Tire Cornering Stiffness [N/deg]	1791

Regarding the rear suspensions, a similar procedure as the front one is applied, although no dependency on the steering input exists. In this case, since it is a rigid axle suspension, the motion of the suspension is derived from the vertical displacement of the centre of the axle and the roll angle. Through a kinematic analysis, the position of each wheel centre is obtained.

Once that the kinematic data of the suspension system is derived, the forces of the spring and damper can be obtained for each time step. Also the contact problem between tires and road can be solved. Thus, all the dynamics of the vehicle are solved.

III. VEHICLE MODEL ACCURACY ANALYSIS

In this section, the accuracy of the proposed approach will be analysed. For that purpose, first, the test vehicle will be presented, and a set of standard maneuvers will be carried out to evaluate the performance of the model in comparison with the data provided by the real vehicle.

A. STUDY CASE: LIGHT DUTY TRUCK

In order to validate the proposed modelling approach, a study case based on a light duty truck (Fig 3) is proposed.

This vehicle has been fully instrumented (IMU, GPS and a robot for steering and throttle/brake pedal commands) and several maneuvers have been executed to extract dynamic behaviour data (see Section III).

Table 1 summarizes the main vehicle parameters, which have been experimentally identified. Note that some of the parameters are confidential and cannot be published. The characterization of the suspension system has been carried out using experimental data. On one hand, the kinematics has been characterized through Kinematics and Compliance (K&C) tests, relating the jounce of the suspension with the different movements of the wheel (lateral, longitudinal, camber, dive and toe). In the case of the front wheels, it is also required the relation between the steering wheel angle with the steer angle of the wheels. On the other hand, for the modelling of the dynamic behaviour, the dampers have been tested and characterized in a specialized testbench. The tests have been carried out with professional equipment at IDIADA's [39] facilities. In addition, the Pacejka's Tire Model parameters have also identified.

Using the experimental identification data, the multibody model detailed in Section II has been defined for this vehicle, and compiled into a C library.

In addition, the powertrain of the real vehicle is composed of a Diesel Internal Combustion Engine (ICE) with a power of 110 kW and a gearbox of 6 different gear ratios. A simplified model has been developed considering the experimental data from the ICE engine (torque/speed curves) and the gears of the vehicle, which includes also the engine brake.

B. MANEUVERS

Four standard maneuvers have been considered, as defined below:

1) **Coast Down:** this maneuver is one of the most frequent tests for motor vehicles. It consists of running the vehicle in a straight line, starting at a certain speed and letting it slow down until it stops. The main goal of this test is to evaluate the values of the resistant forces acting on the vehicle at a certain speed and road conditions, to validate the longitudinal dynamics model.

   Please, note that as the real tests have been carried out with different gears, it has been necessary to model the engine brake accordingly to the real ICE (internal combustion engine), as stated in Section III-A.

2) **Step Steer:** the main objective of this test [43] is to asses the lateral dynamic behaviour of a vehicle. Driving in a straight line at constant speed, the steering wheel is rotated as fast as possible to the target angle position, in which the vehicle's lateral acceleration will start to increase as it begins to turn.

3) **Ramp Steer:** the goal of this test [44] is to determine the steady-state circular driving characteristics of the test vehicle, increasing the lateral acceleration. This test is handled at a constant speed and increasing the lateral acceleration. We use a steering ramp input until the limit of adherence is reached.

4) **Frequency response:** This test aims is to determine the lateral transient response behaviour of the test vehicle in the frequency domain. The test covers a steering input frequency range between 0.1 - 4 Hz.

First, the vehicle is driven at the test speed on a straight line. Then, continuous inputs to the steering-wheel at very low frequency are initiated. This input is increased until the maximum frequency. Additionally, the steering-wheel amplitude is maintained as constant as possible throughout the test, and each run is ended with a straight-line driving.

C. VALIDATION SETUP

The aforementioned maneuvers have been first executed by the real vehicle by using the integrated steering robot, which ensures repeatability, and the data from the on-board sensors have been captured.

In a second stage, the input data (steering wheel angle and wheel torques) have been fed to the developed vehicle dynamics model, composed by the powertrain model and the developed multibody model (see Fig. 4). The outputs of the developed virtual vehicle are compared with the results obtained in the real vehicle in order to determine the accuracy of the model.

Please, note that that the dynamic multibody model has been executed with a time step of 1 millisecond in Matlab/Simulink environment.

D. RESULTS

Next, the results for the four maneuvers are analysed.

1) COAST DOWN MANEUVER

The results obtained for the Coast Down maneuver are shown in Fig. 5, in which the vehicle speed for different gears is shown.

As it can be appreciated, an accurate matching between the real longitudinal vehicle speed and the one calculated by the model is achieved. In Table 2 the RMSE obtained for each gear are summarized. From the results it can be seen that the maximum RMSE is 2.04 km/h (0.0235 NRMSE), which can be considered very low value, indicating that the developed vehicle model offers an appropriate accuracy regarding its longitudinal dynamic behaviour.

The speed differences at the end of the tests, with the 2nd to 6th gear, are due to the idle speed controller implemented
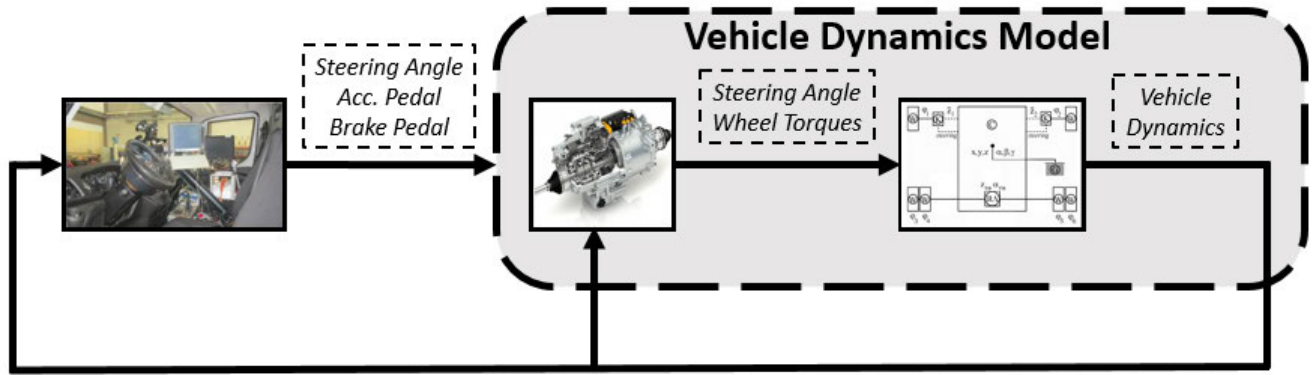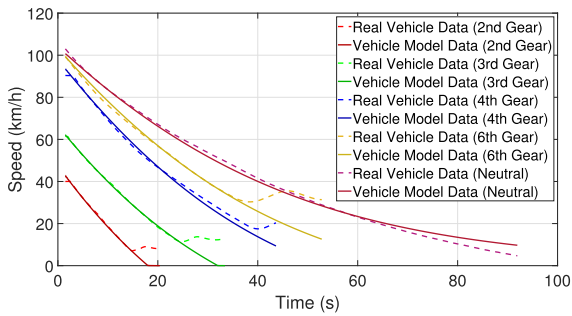
FIGURE 4. Open-loop tests simulation setup.

FIGURE 5. Coast Down maneuver.

TABLE 2. RMSE - coast down maneuver.

Gear	2nd	3rd	4th	6th	Neutral
RMSE [km/h]	0.52	0.32	1.73	1.00	2.04

TABLE 3. RMSE - Step Steer maneuver - 50 km/h.

	Steering Angle degrees		
50 km/h	21	41	67
Lat. Acc. RMSE [m/s^2]	0.0763	0.1523	0.2402
Yaw Rate RMSE [rad/s]	0.0037	0.0034	0.0048

in the real vehicle. This functionality has not been considered in the simulation, as this work does not focus on the powertrain model. Therefore, the RMSE calculation has been made considering that the maneuver ends when this function is activated, except for the test in neutral, as in this case this function is not activated.

2) STEP STEER MANEUVER
This maneuver has been carried out for different steering wheel angles and at different speeds, to evaluate the model's accuracy in a wide range. The results are shown in Figs. 6-11 and in Tables 3-5, where the lateral acceleration and the yaw rate show the accuracy of the proposed model.

The results obtained in this maneuver show the optimal accuracy provided by the developed model. However, it can be appreciated that the error increases with the vehicle speed, as it is approximating to the non-linear region of the tire
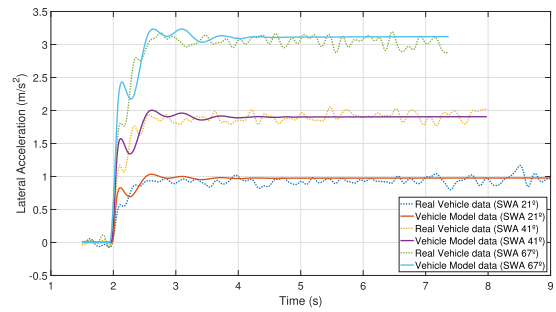
FIGURE 6. Lateral Acc. - Step Steer maneuver - 50 km/h.
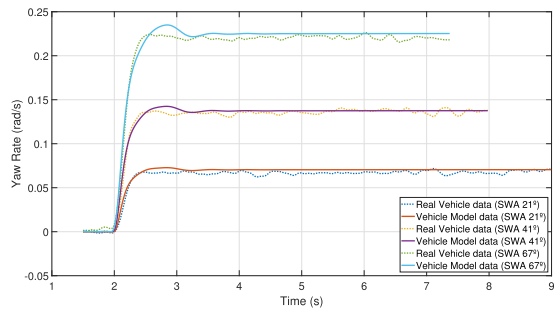
FIGURE 7. Yaw Rate - Step Steer maneuver - 50 km/h.

TABLE 4. RMSE - Step Steer maneuver - 80 km/h.

	Steering Angle degrees		
80 km/h	12	22	32
Lat. Acc. RMSE [m/s^2]	0.0827	0.1575	0.2221
Yaw Rate RMSE [rad/s]	0.0019	0.0020	0.0024

TABLE 5. RMSE - Step Steer maneuver - 100 km/h.

	Steering Angle degrees		
100 km/h	15	23	35
Lat. Acc. RMSE [m/s^2]	0.1332	0.2059	0.3052
Yaw Rate RMSE [rad/s]	0.0025	0.0042	0.0040

model. Therefore, in order to demonstrate the validity of the developed model in extreme cornering conditions, a more hard maneuver, the ramp steer, is executed next.
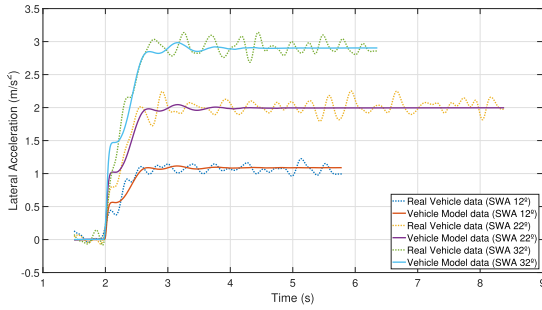
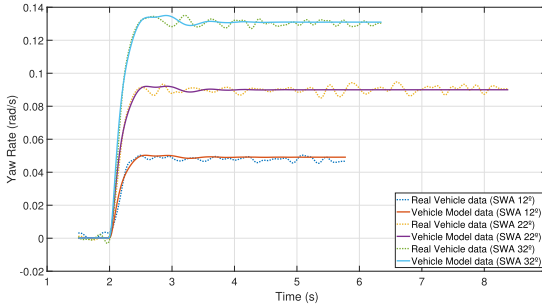**FIGURE 8.** Lateral Acc. - Step Steer maneuver - 80 km/h.

FIGURE 9. Yaw Rate - Step Steer maneuver - 80 km/h.
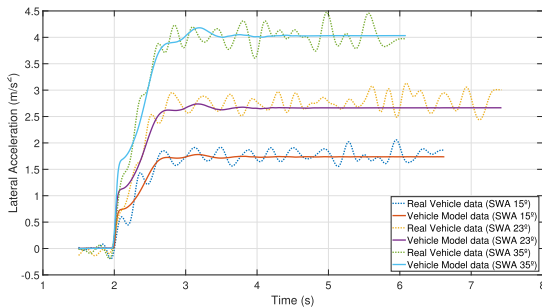

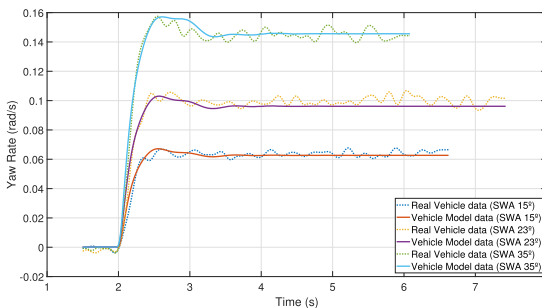**FIGURE 10.** Lateral Acc. - Step Steer maneuver - 100 km/h.

FIGURE 11. Yaw Rate - Step Steer maneuver - 100 km/h.

3) RAMP STEER MANEUVER

Figs. 12-13 show the results obtained for the ramp steer maneuver, which has been carried out at two different speeds (50 km/h and 80 km/h).

As this maneuver takes the vehicle to its limits in terms of lateral dynamics, the variables chosen are the lateral acceleration, the yaw rate and the lateral acceleration with respect to the steering wheel angle.
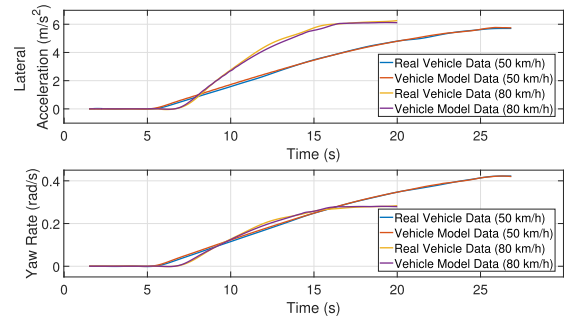
FIGURE 12. Lateral Acc. & Yaw Rate - Ramp Steer maneuver.
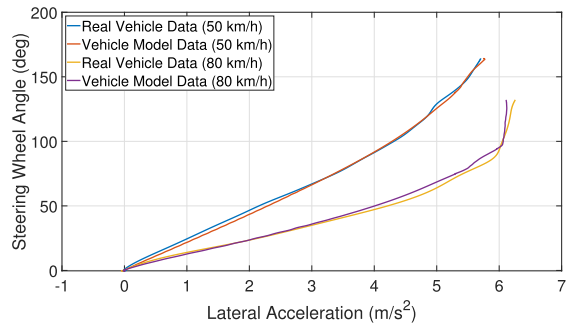
FIGURE 13. Lat. Acc. VS Steering Wheel Angle - Ramp Steer maneuver.

TABLE 6. RMSE - Ramp Steer maneuver.

	Vehicle Speed	
	50 km/h	80 km/h
Lat. Acceleration RMSE [m/s^2]	0.3038	0.3869
Yaw Rate RMSE [rad/s]	0.0004	0.0047

Results show the effectiveness of the developed vehicle model in such a challenging maneuver. The vehicle has reached its maximum lateral acceleration, as it can be appreciated in Fig. 12 and Fig. 13. These figures show that the presented approach provides optimal accuracy in the linear region, and also in the non-linear one, which is reached in the last part of the maneuver, when the maximum lateral acceleration is reached, getting a maximum RMSE of 0.3869 m/s^2 and 0.00047 rad/s.

4) FREQUENCY RESPONSE

Finally, Figs. 14-16 show the results obtained for the frequency response maneuver, which has been carried out at three different speeds (50 km/h, 80 km/h and 100 km/h). The variable selected for the validation is the yaw rate, as it represents effectively the lateral transient behaviours.

Figs. 14-16 show that the simulation results match the data obtained with the real test vehicle, providing very low RMSE values (Table 7).

In conclusion, the low RMSE obtained for all the tested maneuvers demonstrates the optimal accuracy of the proposed approach. Therefore, authors consider that the results validate the proposed modeling approach.
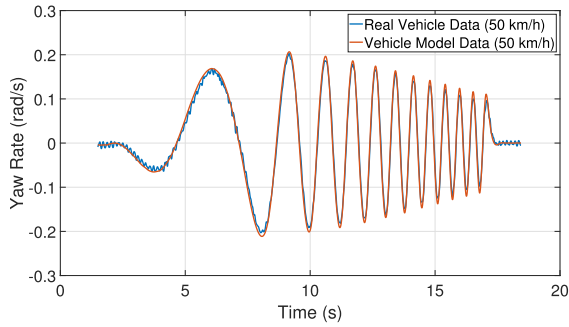
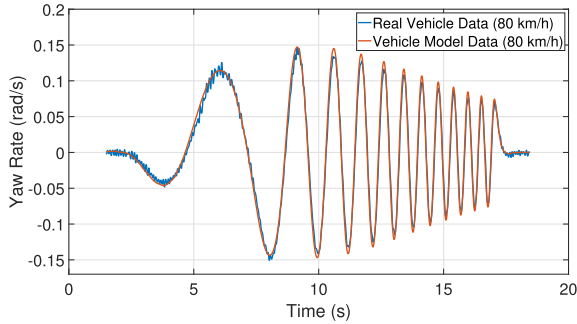**FIGURE 14.** Yaw Rate - Freq. Response maneuver - 50 km/h.

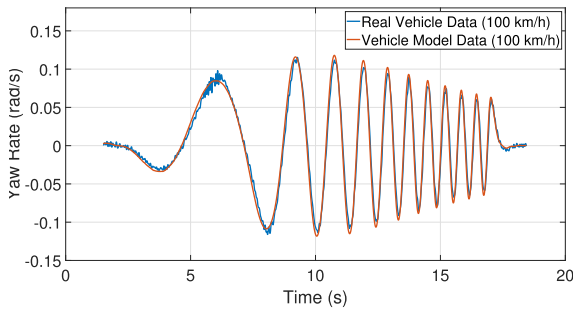**FIGURE 15.** Yaw Rate - Freq. Response maneuver - 80 km/h.

FIGURE 16. Yaw Rate - Freq. Response maneuver - 100 km/h.

TABLE 7. RMSE - Frequency Response maneuver.

	Vehicle Speed [km/h]		
	50	80	100
Yaw Rate RMSE [rad/s]	0.0102	0.0097	0.0090

IV. HiL CAPABILITIES VALIDATION

Hardware in the Loop (HiL) approach is a mandatory feature for a successful testing framework based on simulation, as it allows to reduce significantly the time and cost of the features developments [7], allowing to test not only the code of the ADAS/ADS feature, but also its hardware and communications. However, an appropriate vehicle model (accurate and real time capable) is required in order to ensure the validity of this approach. In this section, a representative example of the implementation of a HiL setup is presented to demonstrate the real-time capabilities of the proposed vehicle modelling approach.

A. HiL SETUP

A simple ADS feature, an autonomous driving controller for the vehicle defined in Section III-A is selected as a study-case. Hence, based on the model validated in Section III, the HiL setup defined in Figure 17 has been defined to test the approach.

Four main blocks are defined in this setup. As defined in Section III, the real vehicle is modelled using two blocks, a powertrain model and the proposed multibody-based model. Both are compiled as a standard C libraries, and are implemented in two National Instruments PXI Industrial PCs (2.3GHz, 8GB RAM), with an execution period of 1ms. Communications between both systems is carried out using TCP/IP protocol.

The autonomous driving controller (virtual driver model) to be tested is based on a Linear Time Variant Model Predictive Controller (LTV-MPC), which is widely known in the literature [40]–[42]. This approach requires a model to predict the future behaviour of the system, hence, a simplified bicycle model [8] for the lateral dynamics and a point mass approach for the longitudinal dynamics is selected. In addition to the physical constraints of the vehicle, a maximum speed of 120 km/h and a maximum lateral acceleration of 6.0 m/s^2 have been selected as output constraints. The developed feature has been implemented in a hardware platform widely used in the Automotive Industry (dSPACE MicroautoBox II [23]), running with an execution period of 10ms. Note that in order to test the corresponding control system, the MicroAutoBox II is connected to the *virtual vehicle*, implemented in the the aforementioned PXIs, using a CAN communication bus.

Finally, an Human Machine Interface and the environment model (with a simplified 3D representation) is executed in a high-end PC. This communicates using TCP/IP with the powertrain and vehicle model PXIs, so that the internal model variables and parameters can be represented, and the 3D visualization updated. In addition, this PC updates the environmental variables to the rest of the mode, such as road friction coefficients and slopes depending on the position of the vehicle. In the defined study-case, two Circuits have been implemented: Silverstone and Barcelona, which will be used to validate the HiL capabilites of the modelling approach.

It is to be noted, that the setup represented in Figure 17 also includes the possibility to implement a Driver in the Loop (DiL) approach, which is also useful to test ADAS features with real drivers.

B. HiL RESULTS AND COMPUTATIONAL COST

Figs 18-19 show the results given by the example automated driving algorithm in the proposed HiL setup. More specifically, Figs. 18a and 19a show the lateral error between the desired trajectory and the one followed by the vehicle; while Figs. 18b and 19b show the vehicle lateral acceleration. Finally, in Fig. 20, the computational cost of the proposed model is shown for this setup.

Results demonstrate that the tested feature performs properly, with low tracking values in the lateral error (Figs. 18a and 19a) and accelerations in the constrained
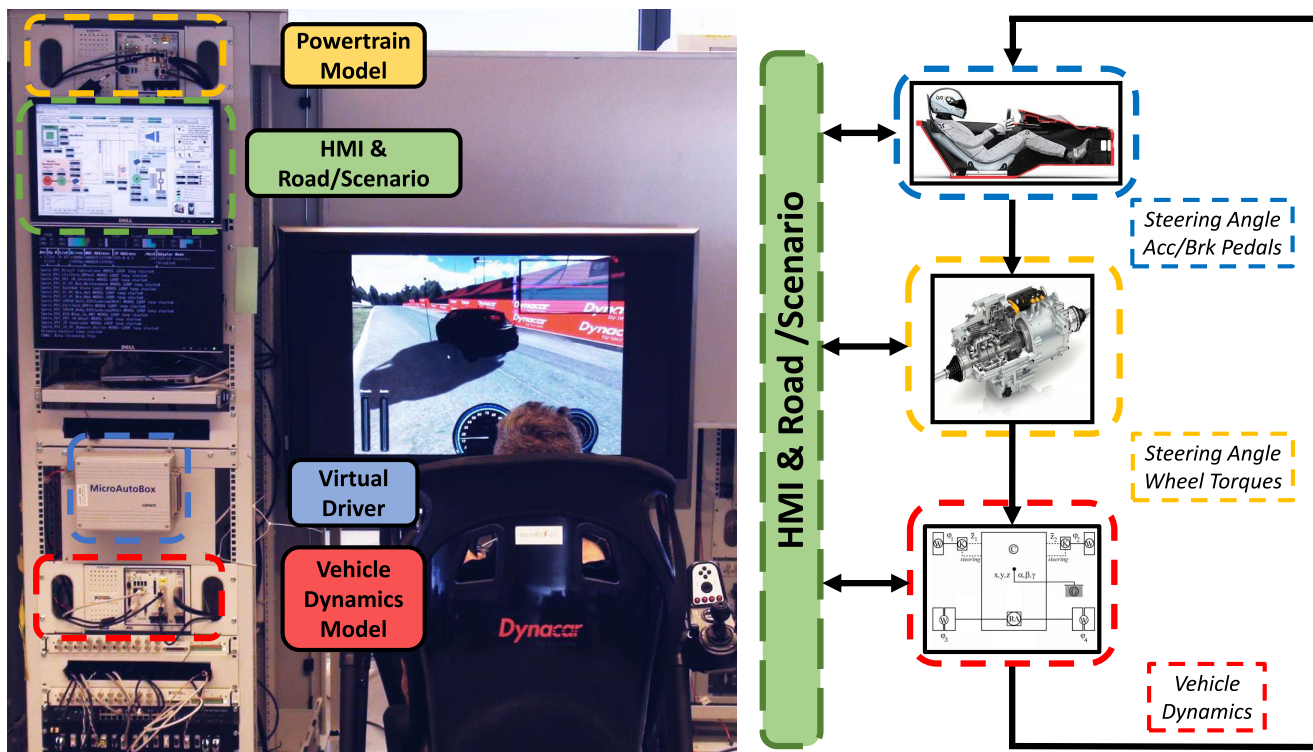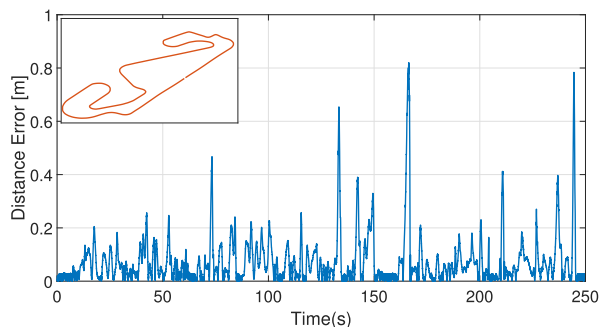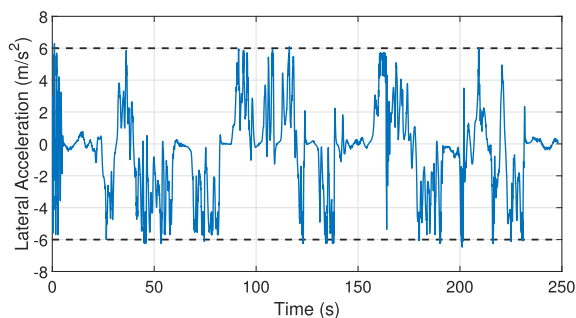
FIGURE 17. HiL Setup based on the proposed multibody vehicle dynamics model.
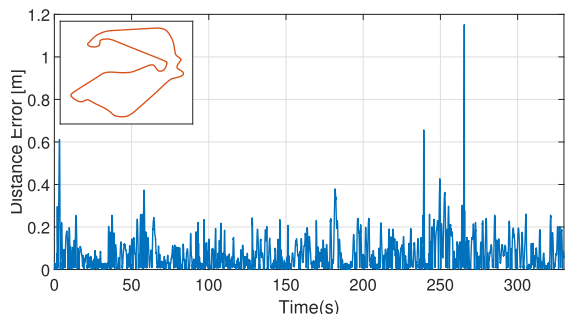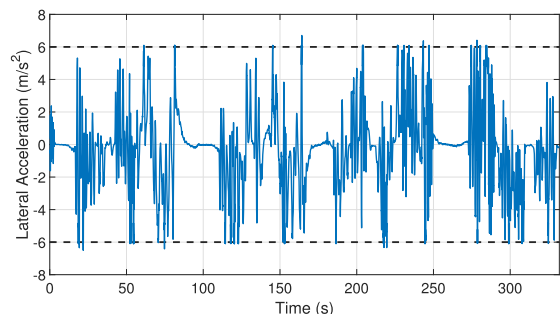

(a) Trajectory Distance Error - Montmelo Circuit

(b) Lateral Acceleration - Montmelo Circuit

FIGURE 18. Driver Model Validation Results for Montmelo Circuit.

(a) Trajectory Distance Error - Silverstone Circuit

(b) Lateral Acceleration - Silverstone Circuit

FIGURE 19. Driver Model Validation Results for Silverstone Circuit.

range (Figs. 18b and 19b). Moreover, the vehicle model mean execution time is 0.22ms for both circuits (Fig 20),

guaranteeing proper real-time performance for the HiL setup, as it is less than 1ms.

(a) Execution Time - Montmelo Circuit

(b) Execution Time - Silverstone Circuit
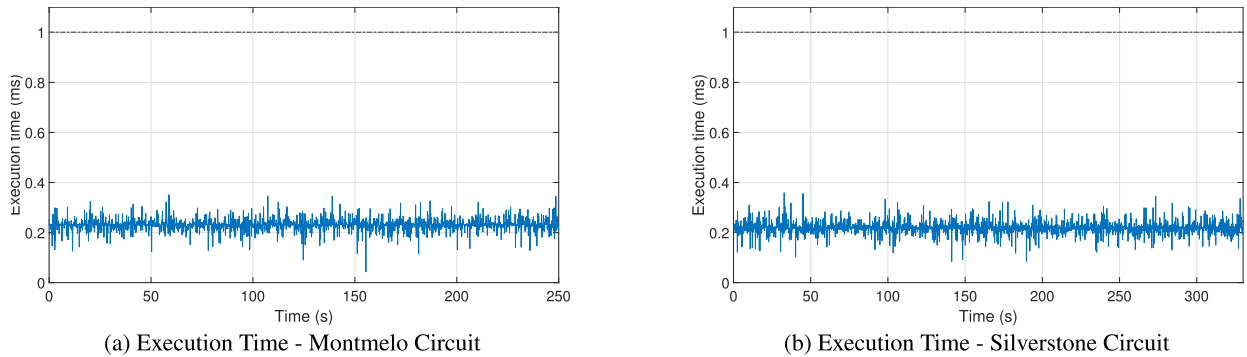
FIGURE 20. Execution time Results.

In fact, this low computational cost means that the proposed approach would be able to be run in a hardware device with lower computation resources, and therefore with lower cost, while keeping the real time capabilities.

V. CONCLUSION

Simulation-based testing is mandatory for the future of ADAS/ADS developments. The cost and lack of flexibility of track tests limit their use when complex control systems need to be tested in vehicles. Moreover, testing frameworks based on simulation allow testing of multiple scenarios at a lower cost. However, developing proper Frameworks is not a trivial task, as they also require a representative vehicle dynamic model, with a proper balance between accuracy, computational efficiency, and flexibility.

In this work, a real time capable vehicle modelling approach is validated thoroughly. The proposed approach provides both accuracy and real-time performance. In order to ensure the maximum flexibility, the approach is coded in standard C, which allows to be run in different hardware.

A double validation has been carried out. First, using a test vehicle (a cargo van), a set of four standard maneuvers are used to compare the real vehicle performance and the simulated one. The real experiments were performed in a dedicated testing facility, to ensure the validity of the data. Results show that the proposed approach presents very low RMS errors (0.38m/s^2 and 0.0047rad/s of lateral acceleration and yaw rate, respectively, in a demanding maneuver, such as the ramp steer at 80 km/h) in comparison with the real vehicle. Second, the developed model is tested in a HiL setup with real-time capabilities. Through the testing of a simple ADS feature, it is demonstrated that the model can be executed in less than 1ms, ensuring real-time performance and proper dynamic simulation.

Future work will include the analysis of more study-cases. For instance, the validation of specific ADAS and functionalities for any type of vehicle, like heavy duty ones.

ACKNOWLEDGMENT

CONFLICT OF INTEREST

The authors declare that they have no conflict of interest.

REFERENCES

[1] A. Roychoudhury, *Embedded Systems and Software Validation* (The Morgan Kaufmann Series in Systems on Silicon). San Mateo, CA, USA: Morgan Kaufmann, 2009.

[2] D. Coulon, *Future of the Automotive Industry, Electronics is the Key*. Fort Worth, TX, USA: Tti Mark, 2014.

[3] *Could be Referenced Like This: Roland Berger Strategy Consultants Consolidation in Vehicle Electronic Architectures*. Accessed: Mar. 5, 2020. [Online]. Available: https://www.rolandberger.com/media/pdf/Roland_Berger_TAB_Consolidation-in-vehicle-electronicarchitectures_20150721.pdf

[4] R. Lattarulo, J. Pérez, and M. Dendaluce, "A complete framework for developing and testing automated driving controllers," *IFAC-PapersOnLine*, vol. 50, no. 1, pp. 258–263, Jul. 2017, doi: 10.1016/j.ifacol.2017.08.043.

[5] C. Granrath, M.-A. Meyer, J. Andert, J. Ewald, R. Klink, C. Stroh, T. Pham, R. Phillips, C. Hettig, L. Santaroni, M. Deppe, and O. Hegazy, "EleMA: A reference simulation model architecture and interface standard for modeling and testing of electric vehicles," *eTransportation*, vol. 4, May 2020, Art. no. 100060, doi: 10.1016/j.etran.2020.100060.

[6] D. E. Conseil, "Extract from the report world electronic industries 2012–2017. General outlook: Towards more professional electronics, a chance for North America and Europe," TTI Eur., Maisach, Germany, Tech. Rep., 2014.

[7] A. Joshi, "Hardware-in-the-loop (HIL) implementation and validation of SAE level 2 autonomous vehicle with subsystem fault tolerant fallback performance for takeover scenarios," in *Proc. SAE Tech. Paper Ser.*, Sep. 2017, pp. 93–125.

[8] H. Guo, D. Cao, H. Chen, C. Lv, H. Wang, and S. Yang, "Vehicle dynamic state estimation: State of the art schemes and perspectives," *IEEE/CAA J. Automatica Sinica*, vol. 5, no. 2, pp. 418–431, Mar. 2018, doi: 10.1109/JAS.2017.7510811.

[9] H. Guo, D. Cao, W. Jin, and H. Chen, "Design of a reduced-order nonlinear observer for vehicle velocities estimation," *IET Control Theory Appl.*, vol. 7, no. 17, pp. 2056–2068, Nov. 2013.

[10] *Carsim*. Accessed: Oct. 1, 2020. [Online]. Available: https://www.carsim.com

[11] J. Garcia de Jalon and E. Bayo, *Kinematic and Dynamic Simulation of Multibody Systems*. New York, NY, USA: Springer, 1994.

[12] M. Arnold, B. Burgermeister, C. Fuhrer, G. Hippmann, and G. Rill, "Numerical methods in vehicle system dynamics: State of the art and current developments," *Vehicle Syst. Dyn.*, vol. 49, no. 7, pp. 1159–1207, Jul. 2011.

[13] S. Bruni, J. P. Meijaard, G. Rill, and A. L. Schwab, "State-of-the-art and challenges of railway and road vehicle dynamics with multibody dynamics approaches," *Multibody Syst. Dyn.*, vol. 49, no. 1, pp. 1–32, May 2020.

[14] Y. Pan, S. Xiang, and A. Mikkola, "An efficient high-order time-step algorithm with proportional-integral control strategy for semirecursive vehicle dynamics," *IEEE Access*, vol. 7, pp. 40833–40842, 2019.

[15] A. Dosovitskiy, G. Ros, F. Codevilla, A. Lopez, and V. Koltun, "CARLA: An open urban driving simulator," 2017, *arXiv:1711.03938*. [Online]. Available: http://arxiv.org/abs/1711.03938

[16] G. Ros, L. Sellart, J. Materzynska, D. Vazquez, and A. M. Lopez, "The SYNTHIA dataset: A large collection of synthetic images for semantic segmentation of urban scenes," in *Proc. IEEE Conf. Comput. Vis. Pattern Recognit. (CVPR)*, Jun. 2016, pp. 3234–3243.

[17] Cognata. (2019). *Cognata Kernel Description*. [Online]. Available: https://www.cognata.com/product/

[18] Vires. (2020). *VTD-Virtual Test Drive Kernel Description*. [Online]. Available: https://www.mscsoftware.com/product/virtual-test-drive

[19] S. Loz. (2019). *Making Autonomous Vehicles Safer Before They Hit the Road*. [Online]. Available: https://www.unrealengine.com/en-US/blog/making-autonomous-vehicles-safer-before-they-hit-the-road

[20] F. Naets, T. Tamarozzi, and W. Desmet, "A system level model reduction approach for flexible multibody systems with parametric Uncertainties," *Procedia IUTAM*, vol. 13, pp. 4–13, Jan. 2015.

[21] *IPG Carmaker*. Accessed: Oct. 1, 2020. [Online]. Available: https://ipg-automotive.com/products-services/simulation-software/carmaker/

[22] *Adams Car*. Accessed: Oct. 1, 2020. [Online]. Available: https://www.mscsoftware.com/product/adams-car

[23] *dSPACE*. Accessed: Oct. 1, 2020. [Online]. Available: https://www.dspace.com/

[24] *ETAS*. Accessed: Oct. 1, 2020. [Online]. Available: https://www.etas.com

[25] *National Instruments*. Accessed: Oct. 1, 2020. [Online]. Available: https://www.ni.com/

[26] *Speedgoat*. Accessed: Oct. 1, 2020. [Online]. Available: https://www.speedgoat.com/

[27] J. Cuadrado, D. Dopico, M. A. Naya, and M. Gonzalez, "Real-time multibody dynamics and applications," in *Simulation Techniques for Applied Dynamics*, vol. 507, G. Maier, J. Salençon, W. Schneider, B. Schrefler, P. Serafini, M. Arnold, and W. Schiehlen, Eds. Vienna, Austria: Springer, 2008, pp. 247–311.

[28] J. Cuadrado, D. Dopico, M. Gonzalez, and M. A. Naya, "A combined penalty and recursive real-time formulation for multibody dynamics," *J. Mech. Des.*, vol. 126, no. 4, pp. 602–608, Jul. 2004.

[29] J. Cuadrado, D. Vilela, I. Iglesias, A. Martín, and A. Peña, "A multibody model to assess the effect of automotive motor in-wheel configuration on vehicle stability and comfort," in *Proc. ECCOMAS Thematic Conf. Multibody Dyn.*, Zagreb, Croatia, 2013, pp. 1083–1092.

[30] M. Dendaluce, I. Iglesias, A. Martin, P. Prieto, and A. Pena, "Race-track testing of a torque vectoring algorithm on a motor-in-wheel car using a model-based methodology with a HiL and multibody simulator setup," in *Proc. IEEE 19th Int. Conf. Intell. Transp. Syst. (ITSC)*, Nov. 2016, pp. 2500–2505.

[31] A. Parra, D. Cagigas, A. Zubizarreta, A. J. Rodriguez, and P. Prieto, "Modelling and validation of full vehicle model based on a novel multibody formulation," in *Proc. IECON - 45th Annu. Conf. IEEE Ind. Electron. Soc.*, Oct. 2019, pp. 675–680, doi: 10.1109/IECON.2019.8926854.

[32] *Road Vehicles—Vehicle Dynamics and Road-Holding Ability*, document ISO 8855, 2011.

[33] *Cosin*. Accessed: Oct. 15, 2020. [Online]. Available: https://www.cosin.eu/products/ftire-product-suite/

[34] *MFTire*. Accessed: Oct. 15, 2020. [Online]. Available: https://www.itwm.fraunhofer.de/en/departments/mf/cdtire.html

[35] W. Hirschberg, G. Rill, and H. Weinfurter, "Tire model TMeasy," *Vehicle Syst. Dyn.*, vol. 45, no. 1, pp. 101–119, Jan. 2007.

[36] G. Rill, "TMeasy—The handling tire model for all driving situations," in *Proc. 15th Int. Symp. Dyn. Problems Mech. (DINAME)*, M. A. Savi, Ed. Buzios, Brazil, 2013.

[37] H. B. Pacejka, *Tyre and Vehicle Dynamics*, 2nd ed. Oxford, U.K.: Butterworth-Heinemann, 2006.

[38] A. J. C. Schmeitz, "A semi-empirical three-dimensional model of the pneumatic tyre rolling over arbitrarily uneven road surfaces," Ph.D. dissertation, Dept. Mech., Maritime Mater. Eng., Delft Univ. Technol., Delft, The Netherlands, 2004.

[39] *IDIADA*. Accessed: Oct. 3, 2020. [Online]. Available: https://www.applusidiada.com/en/

[40] P. Falcone, M. Tufo, F. Borrelli, J. Asgari, and H. E. Tseng, "A linear time varying model predictive control approach to the integrated vehicle dynamics control problem in autonomous systems," in *Proc. 46th IEEE Conf. Decis. Control*, Dec. 2007, pp. 2980–2985.

[41] P. Falcone, H. Eric Tseng, F. Borrelli, J. Asgari, and D. Hrovat, "MPC-based yaw and lateral stabilisation via active front steering and braking," *Vehicle Syst. Dyn.*, vol. 46, no. sup1, pp. 611–628, Sep. 2008.

[42] T. Keviczky, P. Falcone, F. Borrelli, J. Asgari, and D. Hrovat, "Predictive control approach to autonomous vehicle steering," in *Proc. Amer. Control Conf.*, Jun. 2006, p. 6.

[43] *Road Vehicles—Lateral Transient Response Test Methods—Open-Loop Test Methods*, document ISO 7401, 2011.

[44] *Passenger Cars—Steady-State Circular Driving Behaviour—Open-Loop Test Procedure*, document ISO 4138, 1996.
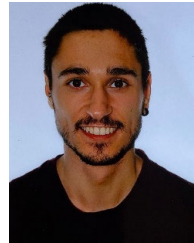
ALBERTO PARRA received the B.Sc. degree in automatics and industrial electronics engineering, the M.Sc. degree in control engineering, automation and robotics, and the Ph.D. degree in vehicle dynamics control systems from the University of Basque Country, in 2015, 2017, and 2020, respectively. He is currently a Researcher with the Tecnalia Research and Innovation Center. His research interests include vehicle dynamics modeling and control, and automated driving.

ANTONIO J. RODRíGUEZ received the degree in mechanical engineering from the University of A Coruna, Spain, in 2015, and the Ph.D. degree from the Laboratory of Mechanical Engineering, University of A Coruna, in 2020. His Ph.D. thesis was on the implementation of car state observers in embedded systems. Since 2016, he received the Ph.D. Grant from the Spanish Government. In 2017, he carried out a four-month pre-doctoral stay at KU Leuven, Belgium. Since 2020, he has been working as a Doctor on applications of multibody dynamics to the automotive field.

ASIER ZUBIZARRETA (Member, IEEE) received the Ph.D. degree in robotics and automatic control systems from the University of the Basque Country, in 2010. He is currently an Associate Professor with the Department of Automatic Control and Systems Engineering, Faculty of Engineering in Bilbao. He has worked in several projects in the areas of robotics, virtual sensors, and model-based predictive control. Since 2012, he has been leading the Formula Student Bizkaia Project. He is focused on the development of virtual sensors and MPC-based controllers for automated driving.

JOSHUÉ PÉREZ (Member, IEEE) received the B.E. degree in electronic engineering from Simon Bolívar University, Venezuela, in 2007, and the M.E. and Ph.D. degrees from the University Complutense of Madrid, in 2009 and 2012, respectively. He has been a Research Leader in automated driving with the Tecnalia Research & Innovation, since 2015. He has more than 11 years of experience in the intelligent transportation system field and 120 publications related to automated driving and advanced driver assistance system.

● ● ●